Carbon Nanotube Electrostatic Biprism: Principle of Operation and Proof of Concept

John Cumings,[1,*] A. Zettl,[1] and M.R. McCartney[2]

[1]*Department of Physics, University of California at Berkeley and Materials Sciences Division, Lawrence Berkeley National Laboratory, Berkeley, CA 94720, USA*
[2]*Center for Solid State Science, Arizona State University, Tempe, AZ 85287-1504, USA*

Abstract: During in situ transmission electron microscopy (TEM) field emission experiments, carbon nanotubes are observed to strongly diffract the imaging TEM electron beam. We demonstrate that this effect is identical to that of a standard electrostatic biprism. We also demonstrate that the nanotube biprism can be used to capture electron-holographic information.

Key words: nanotube, carbon nanotube, biprism, electrostatic biprism, holography, electron holography, field emission

Electron holography is a powerful microscopy technique that can uncover a great wealth of information about biological and inorganic systems. It can give information about the electromagnetic fields in a specimen and has been used to measure the inner potentials of materials (Möllenstedt & Keller, 1957; Lin & Dravid, 1996), interface potentials between materials (Ravikumar et al., 1995), the Aharonov-Bohm effect (Aharonov & Bohm, 1959), and magnetostatic (Matsuda et al., 1989) and electrostatic (Chen et al., 1989) fields in and around samples. A key piece of instrumentation for electron holography is the electrostatic biprism (Möllenstedt & Düker, 1956), which must normally be permanently installed in a transmission electron microscope (TEM). The biprism effectively splits the electron beam into an image wave and a reference wave, which by electrostatic fields are brought to overlap onto one another. In this overlap region, quantum interference fringes occur, from which the phase of the image wave can be directly calculated. From this information, it is possible to extract the details of the electromagnetic fields in a sample.

Biprisms in common use today are constructed by coating ultrasmall quartz fibers with noble metals. The resulting biprisms, although they are quite small by most fabrication standards (approximately 700 nm in diameter), are inconveniently large for holography applications. If a biprism could be made smaller, potential advantages would include reducing the width of the "null region" of the incident beam (the part of the beam that is blocked by the biprism) and thereby increasing the phase coherence of the beam across the bi-

prism. In this article,[1] we describe a set of experiments that demonstrate a nanotube can be used as a biprism for holography experiments and may present significant advantages over traditional biprisms. The experiments stem from the initial observation that under certain conditions, multiwall nanotubes are observed to "light up" during field emission experiments (Cumings et al., 2002; Wang et al., 2002) using specially constructed nanomanipulation stages (Stach et al., 2001) inside the TEM. This effect is shown in Figure 1, where during field emission at 70 V, the nanotubes are clearly observed to become brighter. The effect of nanotube brightening under field emission conditions only occurs when the nanotubes are away from the optimal focus condition, specifically, when the nanotubes are underfocused. If the nanotubes are overfocused, they become larger and darker under field emission conditions. Field emission from nanotubes is induced by biasing the nanotubes at a negative potential with respect to a nearby counterelectrode. If a positive bias is applied to the nanotubes instead, then the overall effect is reversed: When the nanotubes are overfocused, they become bright and when the nanotubes are underfocused, they become dark.

The effect is a direct result of diffraction of the TEM imaging beam by the electrostatic fields around the nanotube. When the nanotube is at a strong negative bias, the electron beam is repelled, and when the nanotube is at a strong positive bias, the beam is attracted. This effect is depicted in Figure 2. The bright nanotubes in the TEM

---

[1]Experiments were performed both at the National Center for Electron Microscopy at Lawrence Berkeley National Laboratory and at the Center for High Resolution Electron Microscopy at Arizona State University. All experiments were performed on Phillips CM-200 microscopes operated at 200 keV or 115 keV.
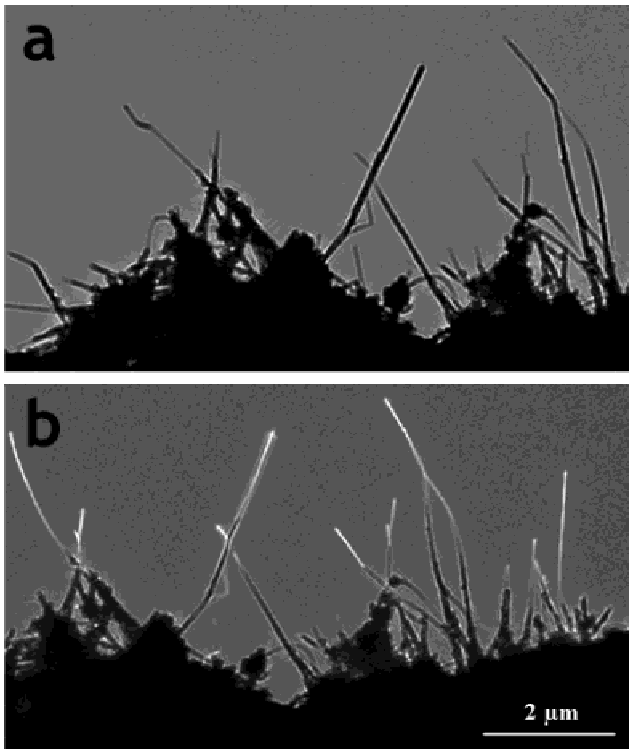
Figure 1. Field emission from nanotubes as observed in the TEM. The images are underfocused (primarily for improved contrast). In **a**, the nanotubes are at ground potential. In **b**, the nanotubes are negatively biased relative to a counterelectrode in the field-emitting regime.
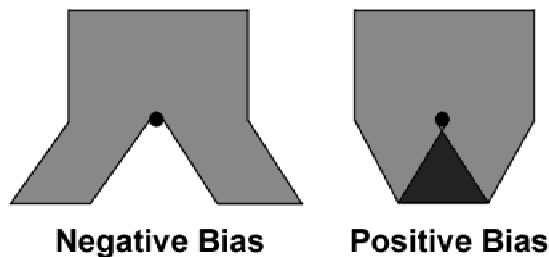

Figure 3. A basic ray diagram of electron optics for a TEM.

Figure 2. The basic effect on the TEM imaging beam (ignoring the effects of electron optics) of the field enhancement around nanotubes under strong bias conditions.

Figure 4. Ray diagrams for a negatively biased nanotube for various objective lens focus conditions.

image are caused when the electron beam overlaps onto itself due to an interaction with the fields in the vicinity of the field-emitting nanotube. To understand how the simple effect of Figure 2 gives rise to the complex behavior outlined in the previous paragraph, an explanation of the basics of electron optics is necessary. A ray diagram showing the operation of a TEM is shown in Figure 3 (Fultz & Howe, 2001). In brief, the effect of the lens is that all sets of parallel rays emitting from the specimen are brought to common points in the back focal plane of the microscope, where a diffraction pattern of the specimen is exhibited. This then
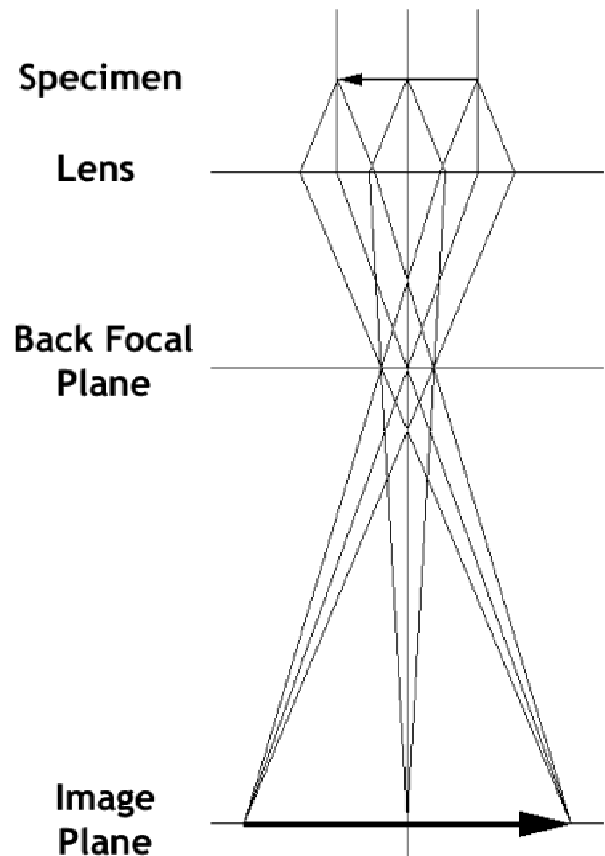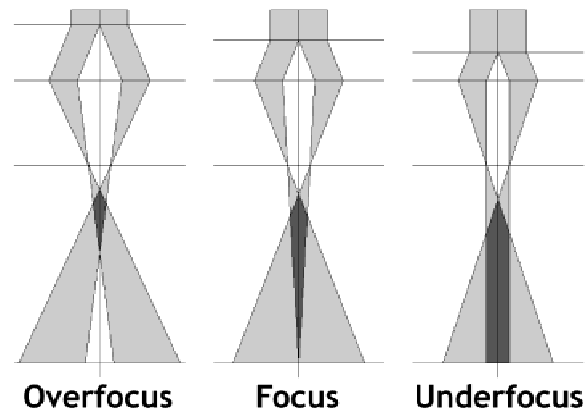
leads to an image plane at a lower position in the microscope column, where a direct image of the specimen can be recorded under optimum focus conditions.

Ray diagrams for the case of a negatively biased nanotube are shown in Figure 4. In this figure, the nanotube is understood to be at the specimen plane in the ray diagram. As is shown, the influence of the electric-field-induced
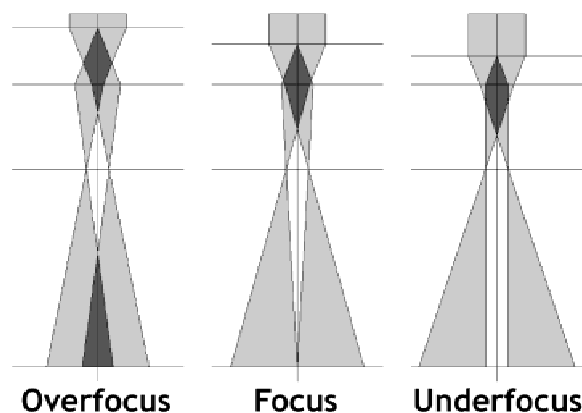
Figure 5. Ray diagrams for a positively biased nanotube for various objective lens focus conditions.
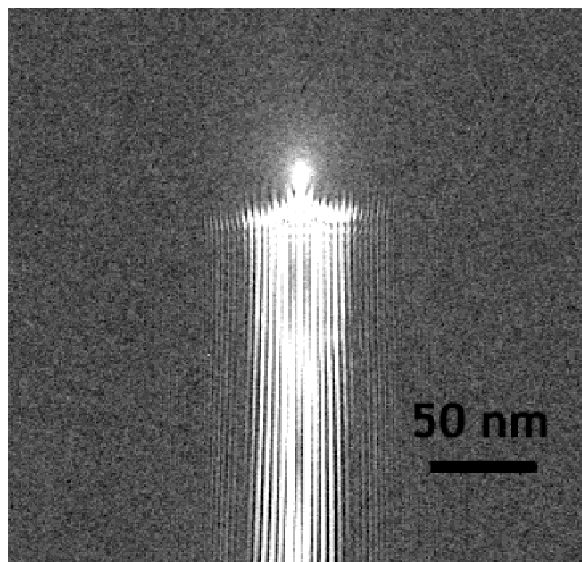

Figure 6. A high-resolution TEM micrograph of a field-emitting nanotube.

diffraction is different depending on whether the nanotube is overfocused or underfocused. When the nanotube is underfocused, the beam is caused to converge and overlap onto itself, thus producing a brightening of the nanotube in the image plane. When the nanotube is overfocused, the beam is caused to diverge, producing a darkening of the nanotube in the image plane. The alternate case of a nanotube under strong positive bias is shown in Figure 5.

To verify that the brightening effect is indeed caused by electric-field-induced beam convergence, a high-resolution micrograph was taken of a negatively biased, underfocused nanotube, shown in Figure 6. Interference fringes can clearly be seen, indicating that the brightening is caused by overlap of the TEM imaging beam with itself. One way to demonstrate conclusively that the fringes are indeed caused by quantum interference of the electron beam with itself is to
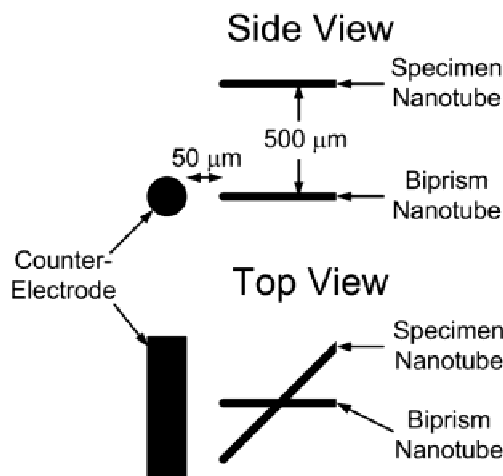

Figure 7. A schematic diagram of the experimental setup used to demonstrate the use of a carbon nanotube as a biprism for electron holography.

calculate the period of the fringes from the convergence angle of the beam and the wavelength of the electrons. Unfortunately, the convergence angle is not precisely known in these measurements. Another method to demonstrate that the fringes are caused by quantum interference is to show that the fringes are shifted when the electron beam undergoes a phase shift. This can be achieved by using the nanotube as a biprism for electron holography.

To use a nanotube as a biprism, another specimen was loaded into the TEM and mounted on the manipulation stage approximately 500 μm above the biprism nanotube. Another nanotube was chosen as the test specimen on which to perform holography. A schematic of the experimental setup is shown in Figure 7. Both nanotubes were held at ground potential relative to the TEM column, and a counter electrode (a 50-μm-diameter gold wire) was placed approximately 50 μm away from the bottom nanotube and biased at +400 V. It was verified with a quick through-focus imaging that the counterelectrode did not cause significant electric fields in the vicinity of the specimen nanotube. An image of the crossing region of the two nanotubes was captured on CCD, shown in Figure 8. Horizontal in the image are clearly seen the interference fringes caused by the nanotube biprism. At an angle to these, the specimen nanotube can be seen. In the path of the specimen nanotube, the electron beam undergoes a phase shift, and in Figure 8a there is a distinct shift of the fringes in the image of the specimen nanotube.[2] Performing a Fourier transform analysis and ex-

---

[2]It is also possible to notice that some fringes appear brighter than others. This is presumably due to the Fresnel fringes of the out-of-focus image of the nanotube biprism, and may have subtle implications for the analysis that follows. These fringes may possibly be removed from the image simply by operating the counterelectrode at higher voltages than were allowed by the experimental setup used here
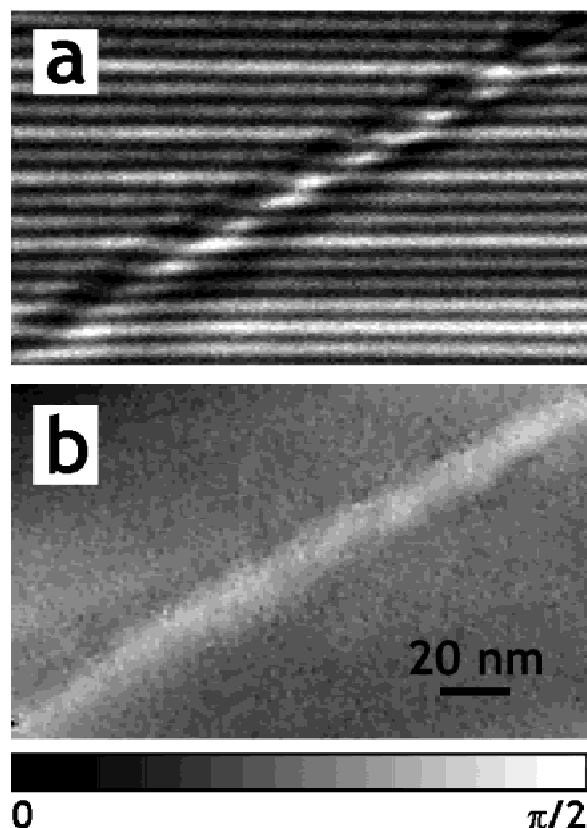
Figure 8. A demonstration of electron holography using a nanotube biprism. In **a**, the hologram is shown. In **b**, the phase extracted from FFT analysis is shown.

tracting the phase of the carrier sidebands yields Figure 8b. In this image, the specimen nanotube can be clearly seen as a 1.1-rad shift from the background phase. This is caused by the mean inner potential of the nanotube due primarily to the positively charged carbon nuclei. Using the phase shift constant (8.77 mrad/V-nm for the 115-kV beam used in this case) and the diameter of the nanotube ($\sim$13 nm), a mean inner potential of $\sim$10 V is extracted for the specimen nanotube. This agrees reasonably well with other experimental results on carbon materials (Lin & Dravid, 1996; Tonomura, 1999; Völkl et al., 1999; Cumings et al., 2002).[3]

Although this demonstrates that a nanotube can, in principle, be used as a biprism, the geometry used in this experiment puts severe restrictions on the types of specimens that can be studied. The placement of the specimen high in the microscope column also limits the ultimate resolution achievable. A nanotube biprism permanently installed in the objective aperture port of the microscope would be much more

useful from a practical point of view, and might even surpass the performance of a more traditional quartz fiber biprism. Both the large diameter of the biprism fiber (typically $\sim$700 nm) and the tendency of the metal coating to sputter off are problems that a nanotube biprism is well equipped to address. However, there would be technical challenges with installing a nanotube at the objective aperture port. The most obvious is simply the size of the nanotube and the physical challenge of accurately positioning the nanotube and mounting it within an aperture. For this, some sort of *in situ* nanomanipulation might be useful, and perhaps the nanotube could be affixed in an aperture with the aid of a scanning electron microscope. It might also be possible, using semiconductor microfabrication techniques, to form an aperture around a nanotube previously isolated on a substrate. An additional problem might be the length of the nanotube. To be a practical biprism, the length should be 10–100 μm, but growing suitable nanotubes of this length could be challenging. It may be possible to instead use vapor-grown semiconductor nanowires (Cui et al., 2001), but the higher mass density and lower Young's modulus of these materials might give rise to increased thermal vibrations of the biprism, similar to those that are observed in TEM images of cantilevered nanotubes (Treacy et al., 1996). It is possible that by using chemical vapor deposition (Endo et al., 1993), nanotubes of the correct length and diameter could be grown. There are additional potential problems with a nanotube biprism that need to be evaluated, such as electron radiation damage to the nanotube and contamination of the nanotube during operation, but this overall problem (of achieving a long, small diameter, stiff, lightweight, conducting fiber) is a fundamental materials question. Carbon nanotubes, owing to their high strength-to-weight ratio and electrical properties, perhaps present the most ideal material for making a nanoscale electrostatic biprism.

ACKNOWLEDGMENTS

REFERENCES

AHARONOV, Y. & BOHM, D. (1959). Significance of electromagnetic potentials in the quantum theory. *Phys Rev* **115**, 485–491.

---

[3]The nanotube imaged here also has an inner diameter of $\sim$2 nm, which should appear as a dark stripe down the axis of the nanotube in the phase map (Lin & Dravid, 1996). Unfortunately, the larger spacing of the interference fringes in Figure 8a ($\sim$5 nm) prevents resolution of the nanotube lumen.

CHEN, J.W., MATTEUCCI, G., MIGLIORI, A., MISSIROLI, G.F., NICHELATTI, E., POZZI, G. & VANZI, M. (1989). Mapping of microelectrostatic fields by means of electron holography—Theoretical and experimental results. *Phys Rev A* **40**, 3136–3146.

CUI, Y., LAUHO, J., GUDIKSEN, M.S., WANG, J.N. & LIEBER, C.M. (2001). Diameter-controlled synthesis of single-crystal silicon nanowires. *Appl Phys Lett* **78**, 2214–2216.

CUMINGS, J., ZETTL, A. & MCCARTNEY, M.R. (2002). Electron holography of field-emitting carbon nanotubes. *Phys Rev Lett* **88**, 056804.

ENDO, M., TAKEUCHI, K., IGARASHI, S., KOBORI, K., SHIRAISHI, M. & KROTO, H.W. (1993). The production and structure of pyrolytic carbon nanotubes (PCNTs). *J Phys Chem Solids* **54**, 1841–1848.

FULTZ, B. & HOWE, J.M. (2001). *Transmission Electron Microscopy and Diffractometry of Materials*. Berlin: Springer.

LIN, X. & DRAVID, V.P. (1996). Mapping the potential of graphite nanotubes with electron holography. *Appl Phys Lett* **69**, 1014–1016.

MATSUDA, T., HASEGAWA, S., IGARASHI, M., KOBAYASHI, T., NAITO, M., KAJIYAMA, H., ENDO, J., OSAKABE, N., TONOMURA, A. & AOKI, R. (1989). Magnetic-field observation of a single flux quantum by electron-holographic interferometry. *Phys Rev Lett* **62**, 2519–2522.

MÖLLENSTEDT, G. & DÜKER, H. (1956). Beobachtungen und Messungen an Biprisma-Interferenzen mit Elektronenwellen. *Zeitschrift für Physik* **145**, 377–397.

MÖLLENSTEDT, G. & KELLER, M. (1957). Elektroneninterferometrische Messung des inneren Potentials. *Zeitschrift für Physik* **148**, 34–37.

RAVIKUMAR, V., RODRIGUES, R.P. & DRAVID, V.P. (1995). Direct imaging of spatially varying potential and charge across internal interfaces in solids. *Phys Rev Lett* **75**, 4063–4066.

STACH, E.A., FREEMAN, T., MINOR, A.M., OWEN, D.K., CUMINGS, J., WALL, M.A., CHRASKA, T., HULL, R., MORRIS, J.W., ZETTL, A. & DAHMEN, U. (2001). Development of a nanoindenter for in situ transmission electron microscopy. *Microsc Microanal* **7**, 507–517.

TONOMURA, A. (1999). *Electron Holography*. Berlin: Springer.

TREACY, M.M.J., EBBESEN, T.W. & GIBSON, J.M. (1996). Exceptionally high Young's modulus observed for individual carbon nanotubes. *Nature* **381**, 678–680.

VÖLKL, E., ALLARD, L.F. & JOY, D.C. (1999). *Introduction to Electron Holography*. New York: Kluwer Academic/Plenum Publishers.

WANG, Z.L., GAO, R.P., DE HEER, W.A. & PONCHARAL, P. (2002). In situ imaging of field emission from individual carbon nanotubes and their structural damage. *Appl Phys Lett* **80**, 856–858.